PHYSICAL REVIEW B **95**, 161115(R) (2017)

Topological defects in Floquet systems: Anomalous chiral modes and topological invariant

Ren Bi,[1] Zhongbo Yan,[1] Ling Lu,[2] and Zhong Wang[1,3,*]

[1]*Institute for Advanced Study, Tsinghua University, Beijing 100084, China*

[2]*Institute of Physics, Chinese Academy of Sciences/Beijing National Laboratory for Condensed Matter Physics, Beijing 100190, China*

[3]*Collaborative Innovation Center of Quantum Matter, Beijing 100871, China*

(Received 1 December 2016; revised manuscript received 23 February 2017; published 26 April 2017)

Backscattering-immune chiral modes arise along certain line defects in three-dimensional materials. Here, we study the Floquet chiral modes along Floquet topological defects, namely, the defects come entirely from spatial modulations of periodic driving. We define a precise topological invariant that counts the number of Floquet chiral modes, which is expressed as an integral on a five-dimensional torus parametrized by (k_x,k_y,k_z,θ,t). This work demonstrates the possibility of creating chiral modes in three-dimensional bulk materials by modulated driving.

DOI: 10.1103/PhysRevB.95.161115

Chiral edge states [1–3] are hallmarks of quantum (anomalous) Hall effects [4–7]. The number of chiral edge modes is determined by the first Chern number [8–10] of the occupied bands of the two-dimensional (2D) systems, which is the best example of bulk-boundary correspondence in topological phases [11–16]. Due to the complete absence of a backscattering channel, transport by chiral modes is dissipationless (as exemplified by the vanishing longitudinal resistivity [4]), which is potentially important in future low-power electronics.

Time-dependent external fields, such as monochromatic lasers, offer highly controllable and tunable tools for creating topological band structures, enlarging the experimental frontiers of topological materials. Recently, considerable progress has been made, both theoretically [17–36] and experimentally [37–41], in understanding periodically driven (Floquet) systems, particularly in connection with topological phases [42–62]. Remarkably, a chiral edge state can exist even if the first Chern number of every bulk band vanishes [48,50,63–65]. This phenomenon is closely related to the absence of a band bottom, which is a distinctive feature of Floquet systems [50].

Interestingly, certain line defects in three-dimensional (3D) crystals also host chiral modes [66–73], which are protected by the second Chern number [74–76]. An experimental realization is lacking so far, because it is challenging to create and manipulate line defects in a controllable manner, therefore, it is worthwhile to study Floquet defects, which can be created by spatial modulation of the driving field [77], without the need for a preexisting static defect. Floquet chiral channels have the advantages that they can be opened or closed, and their spatial locations can readily be tuned, by external driving. Several intriguing questions arise in this direction. How can one determine the number of Floquet chiral modes? How can one create them? In this Rapid Communication, we construct a topological invariant expressed in terms of the evolution operator (inspired by Refs. [50,51]). It is defined as an integral on the five-dimensional (5D) torus parametrized by (k_x,k_y,k_z,θ,t) [Eq. (4)], combining three types of coordinates: momentum, space, and time. We then construct a concrete lattice model, showing that appropriate modulations indeed generate Floquet chiral modes (Fig. 1), in agreement with the prediction from topological invariants.

Topological invariant. We will define a topological invariant that counts the number of Floquet chiral modes along a line defect. Let us take the cylindrical coordinates (r,θ,z) with the defect located along $r=0$, so that the Hamiltonian varies with θ. The topological information can be read from the regions distant from the defect. Sufficiently far away from the defect, the spatial variation of the Hamiltonian is slow, which allows us to define the crystal momentum $\mathbf{k}=(k_x,k_y,k_z)$ [74]. The Bloch Hamiltonian $H(\mathbf{k},\theta,t)$ is an $s\times s$ matrix (s is the number of bands), which is periodic in time, $H(\mathbf{k},\theta,t)=H(\mathbf{k},\theta,t+T)$, with $T=2\pi/\omega$. We can define the time evolution operator $U(\mathbf{k},\theta,t)=\mathcal{T}\exp\left(-i\int_0^t dt' H(\mathbf{k},\theta,t')\right)$, where $\mathcal{T}$ denotes time ordering. The full-period evolution $U(\mathbf{k},\theta,T)$ can be diagonalized as

$$U(\mathbf{k},\theta,T)=\sum_{n=1}^{s}\lambda_n|\psi_n\rangle\langle\psi_n|, \tag{1}$$

and an effective Hamiltonian $H_\varepsilon^{\rm eff}$ can be defined as

$$H_\varepsilon^{\rm eff}(\mathbf{k},\theta)=\frac{i}{T}\sum_n \ln_\varepsilon(\lambda_n)|\psi_n\rangle\langle\psi_n|, \tag{2}$$

where $\ln_\varepsilon$ is the logarithm with a branch cut at $e^{-i\varepsilon T}$, namely, $\log e^{-i\varepsilon T+i0^+}=\log e^{-i\varepsilon T+i0^-}-2\pi i=-i\varepsilon T$ [50,51]. It is apparent that $U(\mathbf{k},\theta,T)=\exp\left[-iH_\varepsilon^{\rm eff}(\mathbf{k},\theta)T\right]$. To have a smooth dependence of $H_\varepsilon^{\rm eff}$ on $\mathbf{k}$ and θ, $e^{-i\varepsilon T}$ must lie in an eigenvalue gap of $U(\mathbf{k},\theta,T)$. The coefficients $\varepsilon_n=(i/T)\ln_\varepsilon(\lambda_n)$ in Eq. (2) are known as quasienergies.

Now we construct a periodic version of U [50,51],

$$U_\varepsilon(\mathbf{k},\theta,t)=U(\mathbf{k},\theta,t)\exp\left[iH_\varepsilon^{\rm eff}(\mathbf{k},\theta)t\right], \tag{3}$$

which satisfies $U_\varepsilon(\mathbf{k},\theta,T)=I=U_\varepsilon(\mathbf{k},\theta,0)$. This property enables us to define the integer topological invariant

$$W(\varepsilon)=\frac{i}{480\pi^3}\int dtd\theta d^3k\,{\rm Tr}\big[\epsilon^{\mu\nu\rho\sigma\tau}\big(U_\varepsilon^{-1}\partial_\mu U_\varepsilon\big)\big(U_\varepsilon^{-1}\partial_\nu U_\varepsilon\big)\times\big(U_\varepsilon^{-1}\partial_\rho U_\varepsilon\big)\big(U_\varepsilon^{-1}\partial_\sigma U_\varepsilon\big)\big(U_\varepsilon^{-1}\partial_\tau U_\varepsilon\big)\big], \tag{4}$$

where the integrating range is $[0,T]\times[0,2\pi]\times{\rm BZ}$ (BZ = Brillouin zone), $\mu,\nu,\rho,\sigma,\tau=k_x,k_y,k_z,\theta,t$, and $\epsilon^{\mu\nu\rho\sigma\tau}=\pm1$ is the Levi-Civita symbol. Given the evolution operator in the

*wangzhongemail@tsinghua.edu.cn

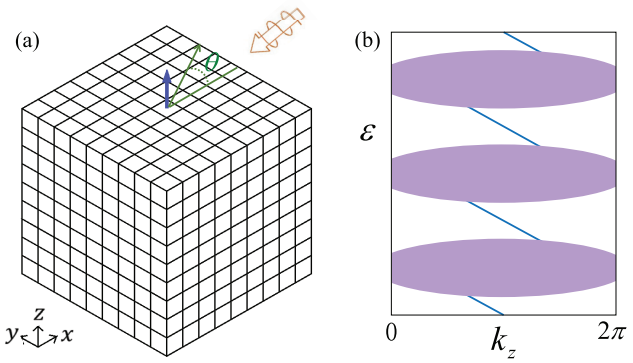

FIG. 1. Sketch. (a) The time-periodic driving is spatially modulated as a function of the polar angle θ, creating a Floquet line defect along $r = 0$ [$r \equiv \sqrt{(x-x_0)^2+(y-y_0)^2}$, $\tan\theta \equiv (y-y_0)/(x-x_0)$; (x_0, y_0) is the location of the defect]. The blue arrow stands for the Floquet chiral modes inside the bulk energy gap. (b) Sketch of the quasienergy bands, with the shadowed region representing the bulk bands, connected by the Floquet chiral modes (blue lines).

5D parameter space (k_x,k_y,k_z,θ,t), Eq. (4) seems to be the only natural topological invariant. The normalization factor in Eq. (4) ensures that W is integer valued [78–81]. As a test, we can show [82] that W reduces in static systems to the second Chern number [74,75], which is known to count the number of chiral modes along the static defects [74,76].

Given two quasienergy gaps $0 \leqslant \varepsilon < \varepsilon' < \omega$, the difference in the branch cut of logarithm causes $H_{\varepsilon'}^{\rm eff}(\mathbf{k},\theta) - H_{\varepsilon}^{\rm eff}(\mathbf{k},\theta) = \omega P_{\varepsilon,\varepsilon'}$, where $P_{\varepsilon,\varepsilon'} = \sum_n' |\psi_n\rangle\langle\psi_n|$ is a projection operator, with $\sum_n'$ denoting the summation for $\varepsilon < \arg(1/\lambda_n)/T < \varepsilon'$. One can define the second Chern number in this subspace, $C_2(\varepsilon,\varepsilon') = (-1/8\pi^2) \int d\theta d^3k\, \mathrm{Tr}[\epsilon^{ijkl} P_{\varepsilon,\varepsilon'}\partial_i P_{\varepsilon,\varepsilon'}\partial_j P_{\varepsilon,\varepsilon'} P_{\varepsilon,\varepsilon'}\partial_k P_{\varepsilon,\varepsilon'}\partial_l P_{\varepsilon,\varepsilon'}]$, in which $i,j,k,l = k_x,k_y,k_z,\theta$. This projection-operator expression is equivalent to the Berry-curvature expression [75]. From the observation $U_{\varepsilon}^{-1}U_{\varepsilon'} = \exp(i\omega t P_{\varepsilon,\varepsilon'})$, one can show that [82]

$$W(\varepsilon') - W(\varepsilon) = C_2(\varepsilon,\varepsilon'), \tag{5}$$

therefore, the Chern number measures the difference between the numbers of chiral modes above and below the band, which, due to the absence of a band bottom, cannot fully determine the number of chiral modes in each gap.

Model. Equation (4) provides clues to the model design. For instance, if the U matrix is 2×2 (namely, two-band), then $W = 0$; thus we consider four-band models. Before investigating spatially modulated driving, we study the homogeneous system first. The Hamiltonian reads

$$H(\mathbf{k},t) = H_0(\mathbf{k}) + H_d(t), \tag{6}$$

where the first part H_0 describes a Dirac semimetal,

$$H_0(\mathbf{k}) = (2t_x \sin k_x\sigma_x + 2t_y \sin k_y\sigma_y + 2t_z \sin k_z\sigma_z) \otimes\tau_z + m(\mathbf{k})\sigma_0 \otimes \tau_x, \tag{7}$$

in which $\sigma_{x,y,z}$ and $\tau_{x,y,z}$ are Pauli matrices ($\sigma_0{=}\tau_0{=}I$), $m(\mathbf{k}){=}B_0{-}B_1\sum_{i=x,y,z}\cos k_i - B_2\sum_{i\neq j}\cos k_i\cos k_j$, with parameters $t_{x,y,z} = B_1 = 1$, $B_2 = 0.1$, $B_0 = 3.6$. Near the Dirac point (0,0,0), $H_0(\mathbf{k}) \approx \sum_i 2t_i k_i \sigma_i \otimes \tau_z$. The second part H_d is driving,

$$H_d(t) = 2D\cos(\omega t)\sigma_0 \otimes (\tau_x\cos\alpha + \tau_y\sin\alpha), \tag{8}$$

with α to be specified shortly. Equation (7) can be written compactly as $H_0 = \mathbf{d}\cdot\Gamma \equiv \sum_{\mu=1}^{5} d_\mu\Gamma_\mu$, with $d_{1,2,3} = 2t_{x,y,z}\sin k_{x,y,z}$, $d_4 = m(\mathbf{k})$, $d_5 = 0$, $\Gamma_{1,2,3} = \sigma_{x,y,z}\otimes\tau_z$, $\Gamma_4 = \sigma_0\otimes\tau_x$, and $\Gamma_5 = \sigma_0\otimes\tau_y$. The bands of H_0 are $E_\pm(\mathbf{k}) = \pm d(\mathbf{k})$ ($d \equiv |\mathbf{d}|$).

Physically, we can regard $\sigma_z = \pm1$ as spin states, and $\tau_z = \pm1$ as two orbitals. Suppose that $\tau_z = \pm1$ orbitals have adjacent orbital-angular-momentum quantum numbers, say, $m_z = 0,1$, respectively, then $H_d(t)$ describes the electric-dipole coupling to an alternating electric field in the $(\cos\alpha, \sin\alpha, 0)$ direction, therefore, $H_d(t)$ can be provided by a linearly polarized laser beam with frequency ω.

We shall calculate the quasienergy bands $\varepsilon_n(\mathbf{k})$ in the frequency domain. Employing the Fourier expansion [42,44,50], $|\psi_n(\mathbf{k},t)\rangle = e^{-i\varepsilon_n(\mathbf{k})t}\sum_{m=-\infty}^{\infty}|\phi_n^{(m)}(\mathbf{k})\rangle e^{im\omega t}$, the Schrödinger equation $i\partial_t|\psi_n(\mathbf{k},t)\rangle = H(\mathbf{k},t)|\psi_n(\mathbf{k},t)\rangle$ becomes

$$\sum_{m'}\mathcal{H}_{mm'}(\mathbf{k})\left|\phi_n^{(m')}(\mathbf{k})\right\rangle = \varepsilon_n(\mathbf{k})\left|\phi_n^{(m)}(\mathbf{k})\right\rangle, \tag{9}$$

in which $\mathcal{H}_{mm'} = m\omega\delta_{mm'}\mathbf{1} + H_{m-m'}$, with $H_m = \frac{1}{T}\int_0^T dt e^{-im\omega t}H(t)$. The Floquet Hamiltonian in Eq. (9) is an infinite-rank matrix,

$$\mathcal{H}(\mathbf{k}) = \begin{pmatrix} \cdots & & & & \\ & H_0+\omega & H_1 & H_2 & \\ & H_{-1} & H_0 & H_1 & \\ & H_{-2} & H_{-1} & H_0-\omega & \\ & & & & \cdots \end{pmatrix}. \tag{10}$$

The spectrum of Eq. (10) is mathematically equivalent to the Wannier-Stark ladder [83], whose eigenstates are localized in m, namely, each eigenfunction decays as $\exp(-|m-m_0|\omega/\Lambda)$ for a certain m_0 (Λ is the system's typical energy scale). Therefore, we can truncate $\mathcal{H}(\mathbf{k})$ to $\mathcal{H}^{(N)}(\mathbf{k})$, which contains $N\times N$ blocks, with H_0 being the central block. As long as $N \gg \Lambda/\omega$, the truncation errors for eigenfunctions not close to the upper and lower truncation edges (approximately at $\pm N\omega/2$) are exponentially small and thus negligible.

In our model, $H_{\pm1} = D\sigma_0\otimes(\tau_x\cos\alpha + \tau_y\sin\alpha)$ and $H_{\pm2,\pm3,\ldots} = 0$. When $D = 0$, the Floquet bands are given by $E_\pm(\mathbf{k}) + m\omega$. Adjacent Floquet bands cross at the resonance surface [Fig. 2(a)] defined by $d(\mathbf{k}) = \omega/2$, namely, $E_-(\mathbf{k}) + \omega = E_+(\mathbf{k})$. Nonzero D hybridizes adjacent Floquet bands, say, $m = 0$ and $m = 1$, generating a quasienergy gap near $\varepsilon = \omega/2$. Hereafter we take $\omega = 4.2$ and $D = 0.6$ for concreteness. The Floquet bands for $\alpha = 0$ are shown in Fig. 2(b). Other values of α give qualitatively similar bands.

Floquet chiral modes. Equation (4) implies that suitable spatial modulations of the driving H_d (with H_0 unchanged) can generate Floquet chiral modes. To this end, we take in Eq. (8) $\alpha = n\theta$ (n is a nonzero integer; θ is the polar angle), thus

$$H_{\pm1} = D\sigma_0\otimes[\cos(n\theta)\tau_x + \sin(n\theta)\tau_y], \tag{11}$$

creating a Floquet line defect at $r = 0$ [Fig. 1(a)]. Taking the previous physical interpretation of the model, these defects can be generated by cylindrical vector beams of the laser [84], in which the spatial modulation in polarization takes exactly the desired form.

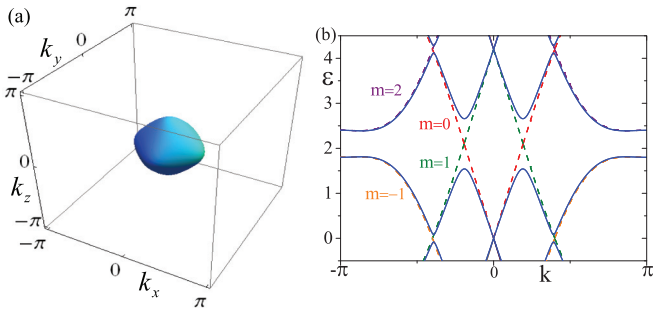

FIG. 2. (a) The resonance surface $d(\mathbf{k}) = \omega/2$, where the $m = 0$ and $m = 1$ Floquet bands cross each other (when $D = 0$). (b) Floquet bands along the 111 direction ($k_x = k_y = k_z = k$) for $D = 0$ (dashed curves, with the Floquet index m marked), and $D = 0.6$ (solid curves). All bands are doubly degenerate.

We calculated the quasienergy bands for a sample with an open boundary in the x-y directions, with a defect at the center. In the calculation, $H_0(\mathbf{k})$ is Fourier transformed to the real space (H_d contains θ but not $\mathbf{k}$, thus it is already a real-space expression). For $n = 1$, the quasienergy bands are shown in Fig. 3(a), in which two in-gap chiral modes with degenerate quasienergies are found (the inessential twofold degeneracy can be lifted by breaking crystal symmetries). The wave-function profiles indicate that they are sharply localized around the line defect at $r = 0$ [Fig. 3(b)].

For the $n = 2$ defect, we find four chiral modes [two thick blue curves in Fig. 3(c), each being doubly degenerate] propagating in the same direction as in $n = 1$. In addition to these chiral modes, there are several trivial nonchiral defect modes, which are shown as dashed curves. The profiles of the four chiral modes are shown in Figs. 3(d) and 3(e). Summarizing the results for $n = 1,2$ and other n's we calculated, the number of chiral modes in the $\omega/2$ bulk gap is

$$M = -2n, \tag{12}$$

where the $\pm$ sign stands for the $\pm z$ direction of propagation. The factor "2" here is somewhat unexpected. Recall that when Dirac fermions are coupled to a complex-valued scalar field [66,67,85], which serves as a Dirac mass, the chiral-mode number of a line defect equals the winding number of the complex scalar field, without a factor of 2. Our Floquet model differs in that the resonance surface is two dimensional, thus the defect here belongs to a different class, to which our intuition from gapping out zero-dimensional Dirac points is inapplicable.

Equation (12) can be predicted by the topological invariant Eq. (4). The calculation of $W(\omega/2)$ simplifies significantly in the small D regime. It is sufficient to focus on this regime because W, as an integer by definition, is insensitive to the value of D, moreover, D is indeed small in current experimental setups [86]. When $D \ll 1$, $H_d(t)$'s contribution to the integral in Eq. (4) is negligible in most of the region of the $(\mathbf{k},\theta,t)$ space, except in small neighborhoods of singular points, where $\frac{\partial U_{\omega/2}}{\partial D}|_{D=0}$ diverges, so that even an infinitesimal D can have non-negligible contribution to the integral. From Eq. (3), we see that such a divergence can originate only from the branch cut in the definition of $H^{\text{eff}}_{\omega/2}(\mathbf{k},\theta)$. To obtain $H^{\text{eff}}_{\omega/2}$,

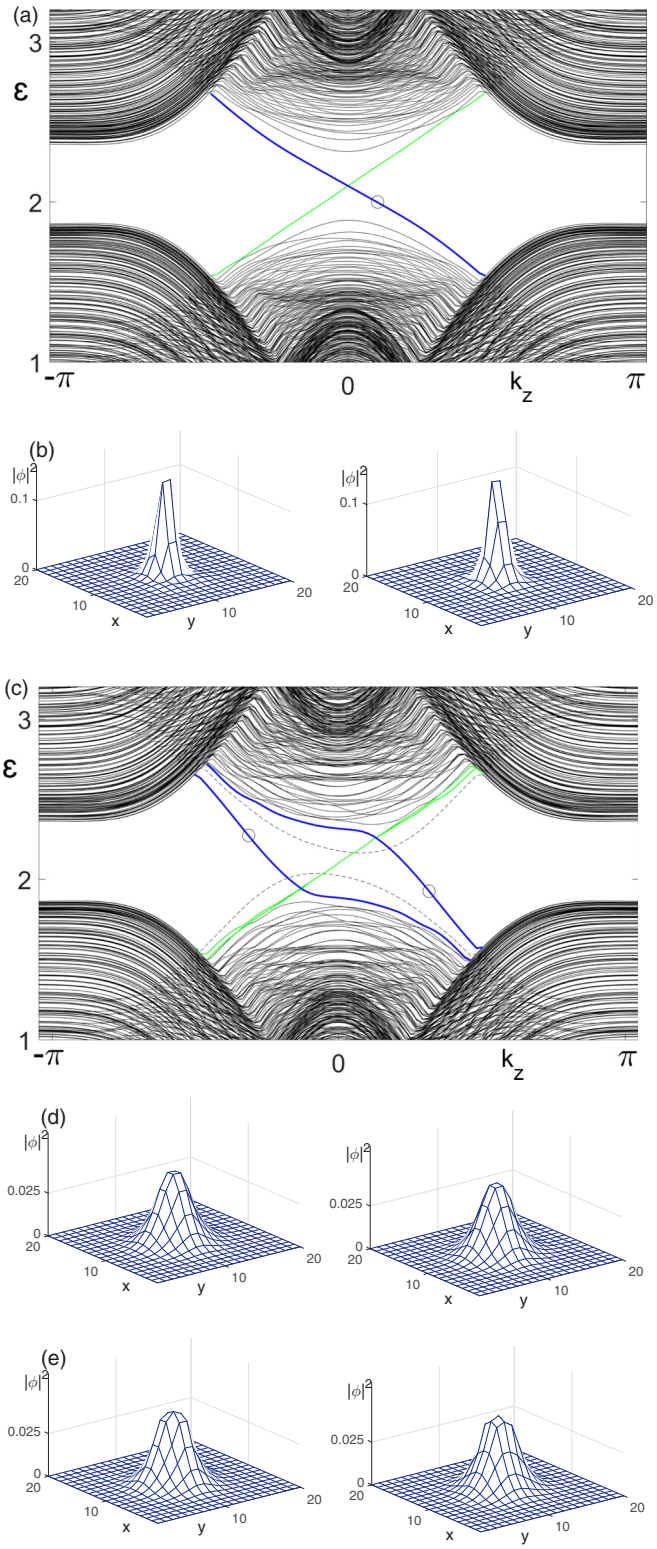

FIG. 3. (a) Quasienergy bands $\varepsilon(k_z)$ of an open-boundary sample with a Floquet line defect (with $n = 1$). The system size is $L_x \times L_y \times L_z = 20\times20\times\infty$. The thick blue curve represents the chiral modes localized near $r = 0$, while the thin green curve represents the back-propagating modes at the system boundary. Each band is doubly degenerate. (b) The wave-function profiles of the two energetically degenerate chiral modes at $k_z = 0.1\pi$ [indicated by an open circle in (a)]. (c) shows bands for the $n = 2$ defect. The chiral-mode profiles at $k_z = 0.3\pi$ and -0.3π are shown in (d) and (e), respectively.

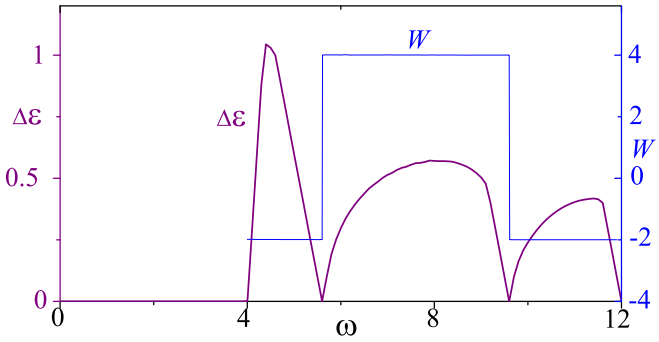

FIG. 4. The bulk quasienergy gap $\Delta\varepsilon$ around $\omega/2$ and the topological invariant $W(\omega/2)$ for $n = 1$ (in the gapped regime).

we recast the full-period evolution operator into [82]

$$U(\mathbf{k},\theta,T) = R(T)\mathcal{T}\exp\left(-i\int_0^T dt\, R^\dagger(t)[H(t) - i\partial_t]R(t)\right) \times R^\dagger(0),$$

which is valid for any choice of unitary matrix $R(t)$. Motivated by the rotating-wave approximation [43,87], we take $R(t) = \exp[\frac{i\omega t}{2}(I - \hat{\mathbf{d}}\cdot\Gamma)]$ ($\hat{\mathbf{d}} = \mathbf{d}/d$), which satisfies $R(T) = R(0) = I$. Taking its logarithm, we can obtain a formula for $H^{\rm eff}_{\omega/2}$ [82],

$$H^{\rm eff}_{\omega/2} = -\frac{\omega}{2}\hat{\mathbf{d}}_{\rm R}\cdot\Gamma + \cdots, \tag{13}$$

which is accurate to the leading order of D. Here, $\hat{\mathbf{d}}_{\rm R} = \mathbf{d}_{\rm R}/|\mathbf{d}_{\rm R}|$ and

$$\mathbf{d}_{\rm R} \equiv \left(d - \frac{\omega}{2}\right)\hat{\mathbf{d}} + \bar{\mathbf{D}}, \tag{14}$$

with $\bar{\mathbf{D}} \equiv \mathbf{D} - (\mathbf{D}\cdot\hat{\mathbf{d}})\hat{\mathbf{d}}$ being the perpendicular (to $\mathbf{d}$) part of $\mathbf{D} = (0,0,0,D\cos n\theta, D\sin n\theta)$. The subscript "R" indicates its close relation to the rotating-wave approximation [43,87].

Let us write $U_{\omega/2}(t) = \tilde{U}(t)\exp[-i\omega t(I + \hat{\mathbf{d}}_{\rm R}\cdot\Gamma)/2]$, then its singular behavior in the $D \to 0$ limit comes solely from the $\hat{\mathbf{d}}_{\rm R}\cdot\Gamma$ term, and $\tilde{U}(t)$ is nonsingular as $D \to 0$. Thus we may simply let $D = 0$ in $\tilde{U}(t)$, and the calculation of the topological invariant becomes mathematically equivalent to that of a static Hamiltonian $(I + \hat{\mathbf{d}}_{\rm R}\cdot\Gamma)/2$, and a straightforward calculation leads to [82]

$$W(\omega/2) = \frac{3}{8\pi^2}\int d\theta d^3k\epsilon^{\mu\nu\rho\sigma\tau}\frac{d_{{\rm R}\mu}}{d_{\rm R}^5}\frac{\partial d_{{\rm R}\nu}}{\partial k_x}\frac{\partial d_{{\rm R}\rho}}{\partial k_y}\frac{\partial d_{{\rm R}\sigma}}{\partial k_z}\frac{\partial d_{{\rm R}\tau}}{\partial\theta}, \tag{15}$$

which can be calculated numerically [88]. It is found that [82]

$$W(\omega/2) = -2n, \tag{16}$$

which precisely matches the number of modes, Eq. (12).

By the same calculation, we can also obtain that $W(-\omega/2) = -2n$, therefore, the second Chern number $C_2(-\omega/2,\omega/2) = W(\omega/2) - W(-\omega/2) = 0$. Thus the Floquet chiral modes in our model have no static analog, i.e., they are *anomalous* in the terminology of Refs. [50,64,65]. In static cases, the chiral-mode number is the sum of all the second Chern numbers of the occupied bands [74], consequently, the chiral mode is absent when every Chern number vanishes.

For completeness, we plot the topological invariant as a function of ω (Fig. 4). The number of chiral modes is consistent with its prediction [82]. The topological invariant is not definable for $\omega < 4.0$, because the quasienergy gap closes around $k_z = \pi$, which is due to the invasion of the $m = -1$ and $m = 2$ Floquet bands into the $\omega/2$ gap. Nevertheless, the chiral modes near $k_z = 0$ persist [82], for the reason that the chiral modes at $\omega/2$ come from the $m = 0$ and $m = 1$ bands. Without the protection of a bulk quasienergy gap, the chiral modes of $\omega < 4.0$ can leak into the bulk sample.

Experimental estimations. For a typical Dirac semimetal, we estimated that the needed laser frequency is in the visible light regime [82]. The penetration depth of the laser into the sample is estimated to be several hundreds of unit cells [82]. If a film with such a thickness is grown, suitable lasers can generate Floquet chiral channels bridging the top and bottom surfaces, which can be measured in transport.

Conclusions. We investigated the possibility of creating chiral modes in 3D materials without static topological defects, by exerting a periodic driving with spatial modulation. We demonstrated it in a concrete model system, and, moreover, we defined a precise topological invariant, which has the feature of combining three classes of variables: momentum, space, and time. Hopefully this work will stimulate further investigations into Floquet topological defects.

Experimentally, this proposal may be realized in Dirac semimetals with appropriate light-matter interactions, as discussed above. If realized, the optically controllable chiral channels may be useful in future high-speed electronics. Our proposal may also be realized in shaking optical lattices [89–95] with suitable spatial modulation, and phononic (or acoustic) systems [96–108], where the mechanical driving can be made to be vortex shaped by design.

Acknowledgments. R.B., Z.Y., and Z.W. are supported by NSFC (No. 11674189). Z.Y. is supported in part by the China Postdoctoral Science Foundation (No. 2016M590082). L.L. is supported by the Ministry of Science and Technology of China (No. 2016YFA0302400) and the National Thousand-Young-Talents Program of China.

[1] R. B. Laughlin, Phys. Rev. B **23**, 5632 (1981).
[2] B. I. Halperin, Phys. Rev. B **25**, 2185 (1982).
[3] X. G. Wen, Phys. Rev. B **41**, 12838 (1990).
[4] K. v. Klitzing, G. Dorda, and M. Pepper, Phys. Rev. Lett. **45**, 494 (1980).
[5] F. D. M. Haldane, Phys. Rev. Lett. **61**, 2015 (1988).

[6] C.-Z. Chang, J. Zhang, X. Feng, J. Shen, Z. Zhang, M. Guo, K. Li, Y. Ou, P. Wei, L.-L. Wang *et al.*, Science **340**, 167 (2013).
[7] R. Yu, W. Zhang, H.-J. Zhang, S.-C. Zhang, X. Dai, and Z. Fang, Science **329**, 61 (2010).
[8] D. J. Thouless, M. Kohmoto, M. P. Nightingale, and M. den Nijs, Phys. Rev. Lett. **49**, 405 (1982).
[9] Q. Niu, D. J. Thouless, and Y.-S. Wu, Phys. Rev. B **31**, 3372 (1985).
[10] Y. Hatsugai, Phys. Rev. Lett. **71**, 3697 (1993).
[11] M. Z. Hasan and C. L. Kane, Rev. Mod. Phys. **82**, 3045 (2010).
[12] X.-L. Qi and S.-C. Zhang, Rev. Mod. Phys. **83**, 1057 (2011).
[13] C.-K. Chiu, J. C. Y. Teo, A. P. Schnyder, and S. Ryu, Rev. Mod. Phys. **88**, 035005 (2016).
[14] A. Bansil, H. Lin, and T. Das, Rev. Mod. Phys. **88**, 021004 (2016).
[15] X. Chen, Z.-C. Gu, Z.-X. Liu, and X.-G. Wen, Phys. Rev. B **87**, 155114 (2013).
[16] X.-G. Wen, *Quantum Field Theory of Many-Body Systems* (Oxford University Press, New York, 2004).
[17] L. E. F. Foa Torres, P. M. Perez-Piskunow, C. A. Balseiro, and G. Usaj, Phys. Rev. Lett. **113**, 266801 (2014).
[18] J. P. Dahlhaus, J. M. Edge, J. Tworzydło, and C. W. J. Beenakker, Phys. Rev. B **84**, 115133 (2011).
[19] A. Gómez-León and G. Platero, Phys. Rev. Lett. **110**, 200403 (2013).
[20] Y. Zhou and M. W. Wu, Phys. Rev. B **83**, 245436 (2011).
[21] P. Delplace, A. Gómez-León, and G. Platero, Phys. Rev. B **88**, 245422 (2013).
[22] R. Wang, B. Wang, R. Shen, L. Sheng, and D. Xing, Europhys. Lett. **105**, 17004 (2014).
[23] L. D'Alessio and M. Rigol, Phys. Rev. X **4**, 041048 (2014).
[24] K. I. Seetharam, C.-E. Bardyn, N. H. Lindner, M. S. Rudner, and G. Refael, Phys. Rev. X **5**, 041050 (2015).
[25] P. Titum, E. Berg, M. S. Rudner, G. Refael, and N. H. Lindner, Phys. Rev. X **6**, 021013 (2016).
[26] N. Goldman, J. Dalibard, M. Aidelsburger, and N. R. Cooper, Phys. Rev. A **91**, 033632 (2015).
[27] H. Wang, L. Zhou, and Y. D. Chong, Phys. Rev. B **93**, 144114 (2016).
[28] H. Hübener, M. A. Sentef, U. de Giovannini, A. F. Kemper, and A. Rubio, Nat. Commun. **8**, 13940 (2017).
[29] D. V. Else, B. Bauer, and C. Nayak, Phys. Rev. Lett. **117**, 090402 (2016).
[30] T. Mori, T. Kuwahara, and K. Saito, Phys. Rev. Lett. **116**, 120401 (2016).
[31] A. Lazarides, A. Das, and R. Moessner, Phys. Rev. Lett. **115**, 030402 (2015).
[32] V. Khemani, A. Lazarides, R. Moessner, and S. L. Sondhi, Phys. Rev. Lett. **116**, 250401 (2016).
[33] L. Zhou, C. Chen, and J. Gong, Phys. Rev. B **94**, 075443 (2016).
[34] M. Thakurathi, A. A. Patel, D. Sen, and A. Dutta, Phys. Rev. B **88**, 155133 (2013).
[35] J. Wang, I. Guarneri, G. Casati, and J. Gong, Phys. Rev. Lett. **107**, 234104 (2011).
[36] G. Usaj, P. M. Perez-Piskunow, L. E. F. Foa Torres, and C. A. Balseiro, Phys. Rev. B **90**, 115423 (2014).
[37] Y. Wang, H. Steinberg, P. Jarillo-Herrero, and N. Gedik, Science **342**, 453 (2013).
[38] F. Mahmood, C.-K. Chan, Z. Alpichshev, D. Gardner, Y. Lee, P. A. Lee, and N. Gedik, Nat. Phys. **12**, 306 (2016).
[39] M. C. Rechtsman, J. M. Zeuner, Y. Plotnik, Y. Lumer, D. Podolsky, F. Dreisow, S. Nolte, M. Segev, and A. Szameit, Nature (London) **496**, 196 (2013).
[40] F. Gao, Z. Gao, X. Shi, Z. Yang, X. Lin, H. Xu, J. D. Joannopoulos, M. Soljačić, H. Chen, L. Lu *et al.*, Nat. Commun. **7**, 11619 (2016).
[41] J. Stehlik, Y.-Y. Liu, C. Eichler, T. R. Hartke, X. Mi, M. J. Gullans, J. M. Taylor, and J. R. Petta, Phys. Rev. X **6**, 041027 (2016).
[42] T. Oka and H. Aoki, Phys. Rev. B **79**, 081406 (2009).
[43] N. H. Lindner, G. Refael, and V. Galitski, Nat. Phys. **7**, 490 (2011).
[44] T. Kitagawa, T. Oka, A. Brataas, L. Fu, and E. Demler, Phys. Rev. B **84**, 235108 (2011).
[45] J.-i. Inoue and A. Tanaka, Phys. Rev. Lett. **105**, 017401 (2010).
[46] Z. Gu, H. A. Fertig, D. P. Arovas, and A. Auerbach, Phys. Rev. Lett. **107**, 216601 (2011).
[47] T. Kitagawa, M. S. Rudner, E. Berg, and E. Demler, Phys. Rev. A **82**, 033429 (2010).
[48] T. Kitagawa, E. Berg, M. Rudner, and E. Demler, Phys. Rev. B **82**, 235114 (2010).
[49] L. Jiang, T. Kitagawa, J. Alicea, A. R. Akhmerov, D. Pekker, G. Refael, J. I. Cirac, E. Demler, M. D. Lukin, and P. Zoller, Phys. Rev. Lett. **106**, 220402 (2011).
[50] M. S. Rudner, N. H. Lindner, E. Berg, and M. Levin, Phys. Rev. X **3**, 031005 (2013).
[51] D. Carpentier, P. Delplace, M. Fruchart, and K. Gawedzki, Phys. Rev. Lett. **114**, 106806 (2015).
[52] T. Kitagawa, M. A. Broome, A. Fedrizzi, M. S. Rudner, E. Berg, I. Kassal, A. Aspuru-Guzik, E. Demler, and A. G. White, Nat. Commun. **3**, 882 (2012).
[53] T. Karzig, C.-E. Bardyn, N. H. Lindner, and G. Refael, Phys. Rev. X **5**, 031001 (2015).
[54] K. Fang, Z. Yu, and S. Fan, Nat. Photon. **6**, 782 (2012).
[55] B. Dóra, J. Cayssol, F. Simon, and R. Moessner, Phys. Rev. Lett. **108**, 056602 (2012).
[56] J. Cayssol, B. Dóra, F. Simon, and R. Moessner, Phys. Status Solidi RRL **7**, 101 (2013).
[57] C.-K. Chan, P. A. Lee, K. S. Burch, J. H. Han, and Y. Ran, Phys. Rev. Lett. **116**, 026805 (2016).
[58] Z. Yan and Z. Wang, Phys. Rev. Lett. **117**, 087402 (2016).
[59] A. Narayan, Phys. Rev. B **94**, 041409 (2016).
[60] C.-K. Chan, Y.-T. Oh, J. H. Han, and P. A. Lee, Phys. Rev. B **94**, 121106 (2016).
[61] R. Roy and F. Harper, arXiv:1603.06944.
[62] C. Qu, C. Zhang, and F. Zhang, arXiv:1608.07097.
[63] W. Hu, J. C. Pillay, K. Wu, M. Pasek, P. P. Shum, and Y. D. Chong, Phys. Rev. X **5**, 011012 (2015).
[64] D. Leykam, M. C. Rechtsman, and Y. D. Chong, Phys. Rev. Lett. **117**, 013902 (2016).
[65] S. Mukherjee, A. Spracklen, M. Valiente, E. Andersson, P. Öhberg, N. Goldman, and R. R. Thomson, Nat. Commun. **8**, 13918 (2017).
[66] C. G. Callan and J. A. Harvey, Nucl. Phys. B **250**, 427 (1985).
[67] E. Witten, Nucl. Phys. B **249**, 557 (1985).
[68] Z. Wang and S.-C. Zhang, Phys. Rev. B **87**, 161107 (2013).
[69] R. Bi and Z. Wang, Phys. Rev. B **92**, 241109 (2015).
[70] T. Schuster, T. Iadecola, C. Chamon, R. Jackiw, and S.-Y. Pi, Phys. Rev. B **94**, 115110 (2016).

[71] B. Roy and J. D. Sau, Phys. Rev. B **92**, 125141 (2015).
[72] Y. You, G. Y. Cho, and T. L. Hughes, Phys. Rev. B **94**, 085102 (2016).
[73] Helical defect modes were also studied [109–111].
[74] J. C. Y. Teo and C. L. Kane, Phys. Rev. B **82**, 115120 (2010).
[75] X.-L. Qi, T. L. Hughes, and S.-C. Zhang, Phys. Rev. B **78**, 195424 (2008).
[76] L. Lu and Z. Wang, arXiv:1611.01998.
[77] Y. T. Katan and D. Podolsky, Phys. Rev. Lett. **110**, 016802 (2013).
[78] R. Bott and R. Seeley, Commun. Math. Phys. **62**, 235 (1978).
[79] E. Witten, Nucl. Phys. B **223**, 422 (1983).
[80] Z. Wang, X.-L. Qi, and S.-C. Zhang, Phys. Rev. Lett. **105**, 256803 (2010).
[81] Z. Wang and S.-C. Zhang, Phys. Rev. X **2**, 031008 (2012).
[82] See Supplemental Material at http://link.aps.org/supplemental/10.1103/PhysRevB.95.161115 for details of calculation.
[83] D. Emin and C. F. Hart, Phys. Rev. B **36**, 7353 (1987).
[84] Q. Zhan, Adv. Opt. Photon. **1**, 1 (2009).
[85] R. Jackiw and P. Rossi, Nucl. Phys. B **190**, 681 (1981).
[86] A calculation for general D is in principle possible by discretizing the Brillouin zone [112–114], though it is more time consuming. We shall not pursue it here because the small-D calculation suffices for our purpose.
[87] N. H. Lindner, D. L. Bergman, G. Refael, and V. Galitski, Phys. Rev. B **87**, 235131 (2013).
[88] A shortcut [115] that leads to the same result is to count the number of inverse images of any given point on the 4D unit sphere.
[89] G. Jotzu, M. Messer, R. Desbuquois, M. Lebrat, T. Uehlinger, D. Greif, and T. Esslinger, Nature (London) **515**, 237 (2014).
[90] C. V. Parker, L.-C. Ha, and C. Chin, Nat. Phys. **9**, 769 (2013).
[91] P. Hauke, O. Tieleman, A. Celi, C. Ölschläger, J. Simonet, J. Struck, M. Weinberg, P. Windpassinger, K. Sengstock, M. Lewenstein, and A. Eckardt, Phys. Rev. Lett. **109**, 145301 (2012).
[92] W. Zheng and H. Zhai, Phys. Rev. A **89**, 061603 (2014).
[93] F. Mei, J.-B. You, D.-W. Zhang, X. C. Yang, R. Fazio, S.-L. Zhu, and L. C. Kwek, Phys. Rev. A **90**, 063638 (2014).
[94] K. Jiménez-García, L. J. LeBlanc, R. A. Williams, M. C. Beeler, C. Qu, M. Gong, C. Zhang, and I. B. Spielman, Phys. Rev. Lett. **114**, 125301 (2015).
[95] N. Fläschner, B. Rem, M. Tarnowski, D. Vogel, D.-S. Lühmann, K. Sengstock, and C. Weitenberg, Science **352**, 1091 (2016).
[96] R. Süsstrunk and S. D. Huber, Science **349**, 47 (2015).
[97] E. Prodan and C. Prodan, Phys. Rev. Lett. **103**, 248101 (2009).
[98] P. Wang, L. Lu, and K. Bertoldi, Phys. Rev. Lett. **115**, 104302 (2015).
[99] V. Peano, C. Brendel, M. Schmidt, and F. Marquardt, Phys. Rev. X **5**, 031011 (2015).
[100] S. H. Mousavi, A. B. Khanikaev, and Z. Wang, Nat. Commun. **6**, 8682 (2015).
[101] L. M. Nash, D. Kleckner, A. Read, V. Vitelli, A. M. Turner, and W. T. Irvine, Proc. Natl. Acad. Sci. USA **112**, 14495 (2015).
[102] Z. Yang, F. Gao, X. Shi, X. Lin, Z. Gao, Y. Chong, and B. Zhang, Phys. Rev. Lett. **114**, 114301 (2015).
[103] C. Kane and T. Lubensky, Nat. Phys. **10**, 39 (2014).
[104] X.-F. Li, X. Ni, L. Feng, M.-H. Lu, C. He, and Y.-F. Chen, Phys. Rev. Lett. **106**, 084301 (2011).
[105] J. Paulose, B. G.-g. Chen, and V. Vitelli, Nat. Phys. **11**, 153 (2015).
[106] Z.-G. Chen and Y. Wu, Phys. Rev. Appl. **5**, 054021 (2016).
[107] R. Fleury, A. B. Khanikaev, and A. Alù, Nat. Commun. **7**, 11744 (2016).
[108] Y.-G. Peng, C.-Z. Qin, D.-G. Zhao, Y.-X. Shen, X.-Y. Xu, M. Bao, H. Jia, and X.-F. Zhu, Nat. Commun. **7**, 13368 (2016).
[109] Y. Ran, Y. Zhang, and A. Vishwanath, Nat. Phys. **5**, 298 (2009).
[110] R.-J. Slager, A. Mesaros, V. Juričić, and J. Zaanen, Phys. Rev. B **90**, 241403 (2014).
[111] R.-X. Zhang, J. A. Hutasoit, Y. Sun, B. Yan, C. Xu, and C.-X. Liu, Phys. Rev. B **93**, 041108 (2016).
[112] T. Fukui, Y. Hatsugai, and H. Suzuki, J. Phys. Soc. Jpn. **74**, 1674 (2005).
[113] X. Wang, J. R. Yates, I. Souza, and D. Vanderbilt, Phys. Rev. B **74**, 195118 (2006).
[114] Y.-L. Wu, N. Regnault, and B. A. Bernevig, Phys. Rev. Lett. **110**, 106802 (2013).
[115] Z. Wang, X.-L. Qi, and S.-C. Zhang, New J. Phys. **12**, 065007 (2010).